Food & Function

Accepted Manuscript

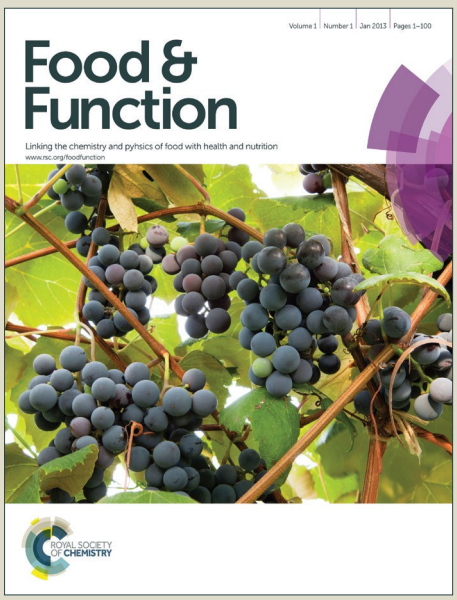

This is an *Accepted Manuscript*, which has been through the Royal Society of Chemistry peer review process and has been accepted for publication.

Accepted Manuscripts are published online shortly after acceptance, before technical editing, formatting and proof reading. Using this free service, authors can make their results available to the community, in citable form, before we publish the edited article. We will replace this *Accepted Manuscript* with the edited and formatted *Advance Article* as soon as it is available.

You can find more information about *Accepted Manuscripts* in the Information for Authors.

Please note that technical editing may introduce minor changes to the text and/or graphics, which may alter content. The journal's standard Terms & Conditions and the Ethical guidelines still apply. In no event shall the Royal Society of Chemistry be held responsible for any errors or omissions in this *Accepted Manuscript* or any consequences arising from the use of any information it contains.

ROYAL SOCIETY OF CHEMISTRY

www.rsc.org/foodfunction

EPA-enriched phospholipids ameliorates cancer-associated cachexia mainly via inhibiting lipolysis

Lei Du[a,b†], Yu-Hong Yang[a,b†], Yu-Ming Wang[b*], Chang-Hu Xue[b], Hideyuki Kurihara[a], Koretaro Takahashi[a*].

Running title: EPA-PL rescues CAC via inhibiting lipolysis

[a] Faculty of Fisheries Sciences, Hokkaido University (3-1-1 Minato-cho, Hakodate, Hokkaido 041-8611, Japan)

[b] College of Food Science and Engineering, Ocean University of China (No.5 Yu-Shan Road, Qingdao, Shandong Province, 266003, People's Republic of China)

[†]These authors contributed equally to this work.

[*]To whom correspondence should be addressed:

Yu-Ming Wang

Tel: +86-532-82032597, Fax: +86-532-82032468. E-mail address: wangyuming@ouc.edu.cn

Koretaro Takahashi

Tel: +81-138-405560, Fax: +81-138-405560. E-mail address: kore@fish.hokudai.ac.jp

Abbreviations

AMPK, AMP-activated protein kinase; ATGL, adipose triglyceride lipase; BAT, brown adipose tissue; BW, body weight; CAC, cancer-associated cachexia; C/EBP *α (β)*, CCAAT/enhancer binding protein alpha (beta); ERK 1/2, extracellular-related kinase 1/2;

EPA-PL, EPA-enriched phospholipids; GLUT4, glucose transporter type 4; HSL, hormone-sensitive lipase; IL-6, interleukins-6; LPL, lipoprotein lipase; NEFA, nonesterified fatty acid; PI3K, phosphoinositide-3-kinase; PGC-1α, peroxisome proliferators-activated receptor gamma coactivator 1α; PPAR γ, peroxisome proliferator-activated receptor gamma; SREBP-1c, sterol regulatory element-binding protein-1c; TG, triacylglycerol; TNF-α, tumor necrosis factor α; UCP2, uncoupling protein 2; WAT, white adipose tissue; ZAG, zinc-α_2-glycoprotein.

Abstract

Excessive loss of fat mass is considered as a key feature of body weight loss in cancer-associated cachexia (CAC). It affects the efficacy and tolerability of cancer therapy and reduces the quality and length of cancer patients` life. The aim of present study was to evaluate the effects of EPA-enriched phospholipids (EPA-PL) derived from starfish *Asterias amurensis* on cachectic weight loss in mice bearing S180 ascitic tumor, TNF-α-stimulated lipolysis in 3T3-L1 adipocytes and to elucidate the possible mechanisms involved. Our findings revealed that oral administration of EPA-PL at 100 mg/kg body weight (BW) per day for 14 days prevented body weight loss in CAC mice by preserving the white adipose tissue (WAT) mass. We found that serum levels of nonesterified fatty acid (NEFA) and pro-inflammatory cytokines such as tumor necrosis factor α (TNF-α) and interleukins (IL)-6 increased in CAC mice but decreased significantly after oral treatment of EPA-PL. In addition, EPA-PL treatment also suppressed the overexpression of several key lipolytic factors and raised the mRNA levels of some adipogenic factors in the WAT of CAC mice. Moreover, treatment of EPA-PL (200 and 400 μM) markedly inhibited TNF-α-stimulated lipolysis in adipocytes. Furthermore, the antilipolytic effects of EPA-PL was stimulated by extracellular-related kinase 1/2 (ERK 1/2) inhibitor PD 98059 and blocked via AMP-activated protein kinase (AMPK) inhibitor compound C and phosphoinositide-3-kinase (PI3K) inhibitor LY 294002. Taken together, these data suggest that the dietary EPA-PL ameliorates CAC mainly via inhibiting lipolysis and at least in part due to recovering the function of adipogenesis.

Key words: EPA-PL, cancer-associated cachexia, TNF-α, white adipose tissue, adipocytes, lipolysis.

1 Introduction

Cancer-associated cachexia (CAC) is a multifactorial wasting syndrome characterized by continuous body weight loss with depletion of adipose tissue and skeletal muscle [1]. Although little is known regarding the mechanisms underlying of adipose atrophy, increased lipolysis in adipose tissue is recognized as an important factor in the progression of CAC [2,3]. Overproduction of adipose triglyceride lipase (ATGL) and hormone-sensitive lipase (HSL), two key rate limiting lipases, have been suggested to be responsible for increased lipolysis [4]. Evidences also suggest that an amount of pro-cachectic substances from malignant tumor or host tissue such as lipid mobilizing factor, zinc-α_2-glycoprotein (ZAG) and circulating pro-inflammatory cytokines such as tumor necrosis factor α (TNF-α) and interleukins (IL)-6 play a crucial role in increased lipolysis in CAC [5]. Increased level of TNF-α has been described to stimulate lipolysis in adipocytes [6], and several studies have proposed that activation of extracellular-related kinase 1 and 2 (ERK 1/2) in adipocytes might be involved in the TNF-α-stimulated lipolysis [7,8]. In addition, the antilipolytic role of AMPK (AMP-activated protein kinase) activation in adipocytes has already been observed [9]. Furthermore, activation of phosphoinositide-3-kinase (PI3K) pathways is also essential for inhibiting lipolysis [10]. On the other hand, recent studies indicate that the vital role of white adipose tissue (WAT) browning in the progression of CAC [11,12]. Peroxisome proliferators-activated receptor gamma coactivator 1α (PGC-1α), a key factor in charge of

regulating the cellular energy metabolism, is expressed in WAT with low level but enriched in metabolically active tissues such as brown adipose tissue (BAT) [13]. Overexpression of PGC-1α in WAT may induce WAT browning and reduce the lipid storage through enhancing the mitochondrial activities in white adipocytes [14]. Moreover, genetic studies suggest that uncoupling protein 2 (UCP2) may also be involved in lipid utilization and energy expenditure [15].

Excessive loss of fat mass could also result from reduced adipogenesis in CAC [16]. The regulation of adipogenesis involves several key transcription factors in a cascade, commencing with increased levels of CCAAT/enhancer-binding proteins beta (C/EBP β), and stimulating the expression of peroxisome proliferator-activated receptor grammar (PPAR γ) and C/EBP α to control the preadipocytes differentiation [14,17,18]. In addition, differentiation is also enhanced through activation of sterol regulatory element-binding protein-1c (SREBP-1c) [19]. Some evidences reveal that lipoprotein lipase (LPL) and glucose transporter type 4 (GLUT 4) also at least in part play a role in the synthesis and storage of triacylglycerol (TG) in adipose tissue [20,21].

Eicosapentaenoic acid (EPA) is an n-3 polyunsaturated fatty acids (PUFAs) found in fish oil and other marine bioresources. Nowadays, EPA are largely marketed in two lipid molecular forms which are TG (EPA-TG) and fatty acid ethyl esters (EPA-EE). Although the most abundant EPA-containing lipid molecular form obtained from marine bioresources is EPA-TG, fisheries by-product sources such as starfish are also rich in EPA-TG and EPA-enriched phospholipids (EPA-PL) which is also called marine phospholipids. EPA is

well-known to have variety of health benefits against several diseases including cancer-associated cachexia [22–25]. However, few studies report the anti-cachectic effects of EPA-PL. Therefore, in this study, we extracted the EPA-PL from starfish *A. amurensis* and investigated its anti-cachectic activity in mice bearing S180 ascitic tumor, a cachexia model which induces excessive loss of body weight. To explore the possible mechanism, we examined the levels of serum biochemical parameters and the relevant pro-inflammatory cytokines in normal and CAC mice. To gain an insight into the molecule mechanism by which EPA-PL alters gene expression of WAT lipid metabolism, the mRNA levels of the genes involved in the lipolysis, lipid utilization and adipogenesis in WAT were determined. Furthermore, to better understand the antilipolytic activity of EPA-PL, we also established the TNF-α-stimulated lipolysis model in 3T3-L1 adipocytes, and lipolysis was evaluated by measuring the amount of glycerol released into media in the presence of several kinase activator and inhibitors.

2 Materials and Methods

2.1 Materials

The starfish *A. amurensis* were collected at the coast of Nemuro, Hokkaido, Japan. Dulbecco's modified Eagle medium (DMEM), Roswell park memorial institute-1640 medium (RPMI-1640), fetal bovine serum (FBS), bovine serum and penicillin-streptomycin were purchased from GIBCO (Grand Island, NY, USA). Sodium 2-(4-iodophenyl)-3-(4-nitrophenyl)-5-(2, 4-disulfophenyl)-2H-tetrazolium (WST-1), 1-methoxy-5-methyphenazinium methylsulfate (1-methoxy PMS) and

2-[4-(2-hydroxyethyl)-1-piperazinyl] ethanesulfonic acid (HEPES) were supplied from Dojindo Laboratories (Kumamoto, Japan). TNF-α, 5-aminoimidazole-4-carboxamide-1-b-D-ribofuranoside (AICAR), LY 294002, PD 98059 and rosiglitazone were provided by Sigma-Aldrich (St. Louis, MO, USA). Compound C was obtained from Merck Millipore (Darmstadt, Germany).

2.2 Preparation of phospholipids from starfish

The total lipids were extracted from the gonad and viscera of starfish following the modified method of Folch *et al* [26] and then mixed with one-fifth volume of 0.15 M NaCl solution. The mixture was placed into a separating funnel and kept at 4 °C for 24 h in the dark and then the chloroform layer was collected and evaporated to dryness under vacuum. Then extracted total lipids were applied to a silica gel column chromatography and eluted with chloroform and acetone to afford neutral lipids and glycolipids. Finally, the column was eluted with methanol to obtain the phospholipids. The purity of phospholipids were confirmed to be 94.5 % on normal phase high performance liquid chromatography coupled with an evaporative light scattering detector (HPLC-ELSD) analysis. The subgroups of phospholipids extracted in this study were separated on thin layer chromatography (TLC) plates using chloroform-methanol-water (65:25:4, v/v/v). Phospholipids were dissolved in ethanol when used in cell experiments and the final ethanol concentration in the medium was adjusted to 0.1 % which was without cytotoxicity. For the animal experiments, the phospholipids was served as liposomes referring to the methods of Hossain *et al* [27] with slight modifications. The mixing molar ratios of the composite lipid classes were phospholipids/cholesterol = 1:1

(mol/mol). The mixtures were dissolved in chloroform and dried to thin film under reduced pressure in a rotary evaporator. The lipid films were hydrated with water to exfoliate lipid bilayers by vigorous vortex mixing for 5 min and were then extruded 21 times through polycarbonate membrane filter (Whatman Inc., Newton, MA, USA) with pore size of 400 nm.

2.3 Fatty acid composition analysis of phospholipids

The phospholipids were converted to methyl ester derivatives following the method of Prevot and Mordret [28] with slight modifications. The dried sample was dissolved in *n*-hexane and 0.2 mL 2N-methanolic-NaOH was added. Then, the mixture was shaken, kept at 50 °C for 30 seconds and 0.2 mL 2N HCl in methanol was added and shaken to neutralize. The mixture was separated by centrifugation at 3000 rpm for 5 minutes. The upper *n*-hexane layer was collected, concentrated, and subjected to gas chromatographic analysis with 0.5 μm PEG-20M liquid phase-coated 40 m × 1.2 mm diameter G-300 column (Chemicals Evaluation and Research Institute, Saitama, Japan) connected to Hitachi 163 gas chromatograph (Hitachi Co. Ltd, Ibaraki, Japan) that was equipped with flame ionization detector. The temperatures of the column, detector, and injection port were 190, 240 and 250 °C, respectively.

2.4 Animals

All animal experimental procedures were approved according to the guidelines of Ethical Committee of Experimental Animal Care at Ocean University of China. Kunming male mice (18-22 g, 6-8 weeks) were purchased from Vital River Laboratory Animal Technology Co. (Beijing, China). The animals were provided with standard chow diet [29] and tap water, and

were kept at a constant temperature of 24 °C, relative humidity of 65 ± 15 % and in a 12 h light-dark cycle.

2.5 Animal protocols

S180 cells (1×10^6 cells in 0.2 mL PBS) were injected into the KM mice via abdominal cavity. The mice were then randomly divided into three groups (8 mice in each group): normal control group, model control group and EPA-PL-treated group. After 24 h, the animals in each group were administered intragastrically of 0.85 % normal saline or the EPA-PL (100 mg/kg BW) once per day for totally 14 consecutive days. Body weight and food intake were recorded daily. At day 15, all the animals were weighed and sacrificed. Blood were collected and serum was separated from whole blood by centrifugation at 1500 × g for 10 min at 4 °C. The ascitic tumor was collected and weighed, and total WAT (including perirenal adipose, epididymal adipose and subcutaneous adipose) were quickly excised, rinsed in ice-cold normal saline. After the tissues were weighted, then were snap-frozen in liquid nitrogen and stored at -80 °C until analysis.

2.6 Measurement of the serum NEFA and cytokines in the serum

Serum NEFA were assessed by the enzymatic assay kits (Wako, Japan). The concentrations of TNF-α and IL-6 in serum were determined by using ELISA kits (R&D system Inc., Minneapolis, MN, USA) following the manufacturer's protocols.

2.7 Real-time polymerase chain reaction analysis

Total cellular RNA was extracted from the 100 mg subcutaneous adipose tissue samples using Trizol reagent (Invitrogen, Carlsbad, CA, USA) according to the manufacture's recommended procedures. One μg RNA from each sample was converted to first strand cDNA using MMLV reverse transcriptase (Promega, Madison, WI, USA) and random primers. Real-time PCR was performed in the Bio-Rad iCycler iQ5 system (Bio-Rad Laboratories, Inc., Hercules, CA, USA). Twenty five μL of the final reaction volume was used for the quantitative real-time PCR assay that consisted of 12.5 μL Maxima SYBR Green qPCR Master mix (Fermentas, Glen Burnie, MD, USA), 10 μM of primers (0.3 μL each of forward and reverse primer), 5.9 μL nuclease-free water, and 6 μL of template. The thermal conditions consisted of an initial denaturation at 95 °C for 10 min followed by 45 cycles of denaturation at 95 °C for 15 s, annealing at 60 °C for 20 s and extension at 72 °C for 30 s, for a final step, a melting curve began at 65 °C and increased 0.5 °C after each 10 s by 61 cycles. Data normalization was accomplished using an endogenous reference β-actin. A dilution curve from one cDNA source using dilutions of 1:2, 1:4, 1:8 and a no-template control was run for each gene. The gene expression level was analyzed by relative quantification using the standard curve method. The sequence of the primers used is described in Table 1.

2.8 Cell culture and differentiation *in vitro*

Mouse 3T3-L1 preadipocytes were obtained from American Type Culture Collection (Rockville, CT, USA) and were cultured in high-glucose DMEM medium, supplemented with 10 % heat-inactivated bovine serum, 100 U/mL penicillin and 100 μg/mL streptomycin at

37 °C in a humidified atmosphere containing 5 % CO_2. Murine sarcoma S180 cells were obtained from Shanghai Cell Bank (Shanghai, China). S180 cells were grown in RPMI-1640 medium, supplemented with 10 % heat-inactivated FBS, 100 U/mL penicillin and 100 μg/mL streptomycin.

The 3T3-L1 preadipocytes were differentiated according to the method of Russell and Tisdale [23] with a slight alterations. Briefly, two days after the cells reached confluence, differentiation was initiated by addition of high-glucose DMEM medium containing 10 % FBS, penicillin-streptomycin, 0.5 mM 3-isobutyl-1-methylxanthine (IBMX), 1 μM dexamethasone (DEX) and 10 μg/mL insulin. After 48 h, cells were cultured with 10 % FBS and 10 μg/mL insulin for a further 48 h. Cells were then cultured in growth medium without insulin for another 4 days when cells were differentiated to mature adipocytes, with medium changes every two days. The differentiation effect was determined by Oil Red O staining.

2.9 WST-1 cell proliferation assay

3T3-L1 preadipocytes were seeded into 96-well plate at 3×10^4 cells/mL in 200 μL growth medium per well. After differentiated as described above, the 3T3-L1 adipocytes were treated with different concentrations of EPA-PL for 48 h. Control cells were treated with the same amount of ethanol. Twenty μL WST-1 (3.26 mg/ml in 20 mM HEPES including 0.2 mM 1-methoxy PMS) was added in each well containing 200 μL medium with cells, and plates were incubated at 37 °C in a 5 % CO_2-humidified incubator for 3 h. The absorbance was subsequently measured at 450-650 nm in each well by using microplate reader

(SpectraMax M5e, Molecular Devices, Sunnyvale, CA, USA). Cell viability was determined at 48 h following the WST-1 cell proliferation assay.

2.10 *In vitro* lipolysis assays

In TNF-α-stimulated lipolysis model [17,30], TNF-α was dissolved in sterile water. AICAR, compound C, LY 294002, PD 98059 and rosiglitazone were dissolved in dimethyl sulfoxide (DMSO). All reagents were prepared in 1000× stock solutions and then diluted to the desired concentrations by culture medium. After 8 days of differentiation, 3T3-L1 adipocytes were incubated with 2 % serum-containing high-glucose DMEM in the absence or presence of 10 ng/mL TNF-*α* in combination with or not with EPA-PL (200 μM), rosiglitazone (25 and 50 μM), AMPK activator AICAR (1 mM), the specific inhibitors such as AMPK inhibitor compound C (20 μM), ERK 1/2 inhibitor PD 98059 (50 μM) and PI3K inhibitor LY 294002 (50 μM) for 48 h. Control cells were treated with the same amount of the corresponding vehicle (ethanol or DMSO). All inhibitors were preincubated 2 h before the addition of TNF-*α* and/or EPA-PL in order to diminish intrinsic kinase activity to a minimum [6].

2.11 Glycerol measurements

Lipolysis was evaluated by measuring the amount of glycerol released into the media. After 48 h, the culture media were centrifuged to remove debris and directly subjected to glycerol concentration measurements using a glycerol cell-based assay kit (Cayman chemical company, Ann Arbor, Michigan, USA). The cells were rinsed with ice-cold PBS, harvested and lysed by lysis buffer. Protein concentration in the lysates were used to normalize the

lipolysis signals. The amounts of glycerol released were determined by using a microplate reader to detect the absorbance at 540 nm following the manufacturer`s instructions of the kit.

2.12 Statistical analysis

All the values in figures are expressed as mean ± standard error of the mean (SEM). All statistical analyses were performed using SPSS software. Data were analyzed using Student`s t-test or Tukey's post hoc test. *P* value less than 0.05 was considered statistically significant.

3 Results

3.1 Fatty acid composition of EPA-PL

As shown in Table 2, EPA-PL extracted from starfish contained 42 % EPA, 6.8 % DHA and 8.8 % arachidonic acid (AA), amounting to 48.8 % n-3 PUFAs. In addition, the TLC result revealed that more than 40 % of the phospholipids was phosphatidylethanolamine (PE) and phosphatidylcholine (PC) was shown to be the second most abundant (36 %).

3.2 Effects of EPA-PL on the physiological parameters, serum NEFA and cytokines in mice

To explore the anti-cachectic effects of EPA-PL on CAC *in vivo*, we investigated the average food intake, carcass weight (without tumor weight) and total WAT in mice. The mice inoculated tumor cells exhibited dramatic weight loss and decrease in food intake at day 15 compared to normal mice. Oral treatment of EPA-PL at 100 mg/kg BW per day for totally 14 consecutive days did not affect the average food intake in mice, but it could induce a notable

253 increase in carcass weight, total WAT mass in CAC mice as compared to CAC model mice
254 (Table 3). These data suggest that EPA-PL can rescue the cachexia *in vivo*.

255 Next, we also measured the levels of serum NEFA in mice. Compared to normal mice,
256 serum NEFA levels increased markedly in CAC mice ($P < 0.01$). But the increase was
257 reversed by EPA-PL treatment (Table 3), suggesting the inhibitory effects of EPA-PL on
258 lipolysis *in vivo*.

259 To further assess whether EPA-PL can affect the pro-inflammatory cytokines secretion
260 in CAC mice, the concentrations of TNF-α and IL-6 in serum were determined by ELISA kits.
261 The serum concentrations of TNF-α and IL-6 were highly elevated in CAC mice ($P < 0.01$)
262 compared to the normal mice (Table 3). Oral administration of EPA-PL could reduce the
263 serum levels of TNF-α and IL-6 noticeably ($P < 0.01$). These results indicate that EPA-PL can
264 ameliorate cachexia through reduction of pro-inflammatory cytokines secretion.

265 **3.3 Effects of EPA-PL on mRNA expression of lipolysis genes in the WAT of**
266 **CAC mice**

267 To elucidate the molecular mechanisms by which oral treatment of EPA-PL ameliorates
268 adipose atrophy in CAC mice, we investigated the mRNA expressions of lipid mobilizing
269 factor ZAG, two key rate limiting lipases ATGL and HSL. As shown in Fig. 1, the mRNA
270 levels of ZAG, ATGL and HSL were up-regulated dramatically in the WAT of CAC mice (P
271 < 0.01). EPA-PL treatment significantly reduced these increases, suggesting the possible
272 pathways for how EPA-PL attenuated lipolysis in CAC mice.

3.4 Effects of EPA-PL on mRNA expression of lipid utilization genes in the WAT of CAC mice

To better understand the regulation of lipid utilization in CAC mice and the actions of EPA-PL, we also measured the mRNA expression of PGC-1α and UCP2. The mRNA levels of PGC-1α and UCP2 were significantly elevated in the adipose tissue of CAC mice, which were remedied remarkably after oral administration with EPA-PL at 100 mg/kg BW per day for totally 14 consecutive days (Fig. 2). These results reveal that EPA-PL can rescue cachexia through regulating the lipid utilization in CAC mice.

3.5 Effects of EPA-PL on mRNA expression of adipogenic genes in the WAT of CAC mice

To verify whether EPA-PL can recover the function of adipogenesis in CAC mice, we also determined the mRNA expressions of several key adipogenic factors. Our data showed that the mRNA levels of C/EBP α, C/EBP β, PPAR γ, SREBP-1c, LPL and GLUT4 in CAC model group were dramatically down-regulated in CAC model mice. However, EPA-PL induced significant recovery of C/EBP α, LPL and GLUT4 but had no effect on C/EBP β, PPAR γ and SREBP-1c expression (Fig. 3). These results demonstrate that the anti-cachectic effects of EPA-PL are at least partly responsible for recovering the function of adipogenesis in CAC mice.

3.6 Effects of EPA-PL on basal and TNF-*α*-stimulated lipolysis and its related pathways

To further clarify whether EPA-PL affects the lipolysis, we investigated the antilipolytic effects of EPA-PL *in vitro*. The result showed that no toxicity was observed in 3T3-L1 adipocytes incubated with EPA-PL at 100, 200 and 400 μM for 48 h (Fig. 4A). As shown in Fig. 4B, the lipid accumulation were blocked after treatment of 10 ng/mL TNF-*α* for 48h in 3T3-L1 mature adipocytes. However, EPA-PL restored the lipid droplets noticeably. These results suggest the inhibitory effects of EPA-PL on TNF-*α*-stimulated lipolysis.

To quantify the antilipolytic effects of EPA-PL on basal and TNF-*α*-stimulated lipolysis, glycerol released into media was determined. EPA-PL did not affect the basal glycerol released into media after 48 h of incubation (Fig. 5A). On the contrary, the adipocytes co-cultured with 25 and 50 μM rosiglitazone (an agonist of PPAR-*γ*) decreased glycerol release significantly after 48 h of culture (Fig. 5B). As we expected, treatment with the pro-inflammatory cytokine TNF-*α* significantly stimulated the glycerol release (increased by 2-fold), while addition of EPA-PL reversed the over-lipolysis which was notably stimulated by TNF-*α* (Fig. 5B). Similarly, the presence of rosiglitazone also suppressed the TNF-*α*-stimulated lipolysis. And the antilipolytic effects of rosiglitazone (50 μM) was stronger than 400 μM EPA-PL which isolated from the starfish in this study ($P < 0.05$).

At last, to elucidate the mechanism by which EPA-PL inhibits TNF-*α*-stimulated lipolysis, we also measured the glycerol release under the presence of EPA-PL (200 μM) and several kinase activator and inhibitors. As shown in Fig. 6A**,** only AICAR (an activator of

AMPK) significantly ($P < 0.01$) reduced the basal lipolysis. And it was also true for TNF-α-stimulated lipolysis in 3T3-L1 adipocytes (Fig. 6B). It must indicate the antilipolytic role of AMPK activation in adipocytes. In addition, AMPK inhibitor compound C blocked the antilipolytic effects of EPA-PL on TNF-α-stimulated lipolysis in 3T3-L1 adipocytes (Fig. 6B). Our finding suggests that AMPK activation is involved in the antilipolytic effects of EPA-PL. Moreover, similar effects on glycerol release were observed after co-treatment with EPA-PL and LY 294002 (an inhibitor of PI3K) on TNF-α-stimulated lipolysis in 3T3-L1 adipocytes (Fig. 6B), suggesting that PI3K is essential in the regulation of TNF-α-stimulated lipolysis in mature adipocytes. Moreover, the inhibition of ERK 1/2 with PD 58059 strongly reduced the glycerol release in the presence of TNF-α and EPA-PL in 3T3-L1 adipocytes as compared to TNF-α in combination with EPA-PL (Fig. 6B). This result reveals that ERK 1/2 activation also plays a vital role for regulating the TNF-α-stimulated lipolysis.

4 Discussion

In the present study, EPA-PL which contains 42 % EPA and amounting to 58.3 % PUFAs was extracted from starfish *A. amurensis*. Nowadays, several studies have suggested that n-3 PUFAs, especially EPA are effective in preventing body weight loss in patients and animals with cancer [22,24,25]. However, little information has been known on the ameliorating effects of EPA-PL on CAC. To the best of our knowledge, only Taylor *et al* [31] reported the anti-cachectic effects of marine phospholipids (containing 67.7 % neutral lipid with 18.8 % EPA and 22.8 % DHA, as well as 28.6 % phosphatidylcholine containing 16.5 % EPA and 33.7 % DHA). But the anti-cachectic action of purified EPA-PL is still unknown. As we know,

TG and fatty acid ethyl ester are hydrophobic compounds, while phospholipids are typical amphiphilic compounds. Therefore, EPA-PL is considered to be much more bioavailable than EPA-TG or EPA-EE. It has been suggested that phospholipids form are more efficient than TG forms in delivering n-3 PUFAs to blood and desired tissues [32–34]. A same molar EPA moiety bound to phospholipids was expected to be more effective in ameliorating CAC than equal or even higher molar EPA moiety bound to TG or fatty acid ethyl ester. Our findings manifested that oral administration of EPA-PL (100 mg/kg/day) for totally 14 consecutive days could suppress the cachectic body weight loss in mice bearing S180 ascitic tumor. Excessive loss of adipose tissue and significant increase of serum NEFA level in CAC mice were also observed in our study, but these changes were reversed by EPA-PL treatment, suggesting the involvement of lipolysis in tumor-induced weight loss and the amelioration of EPA-PL for weight loss by inhibiting lipolysis in CAC mice. On the other hand, dietary EPA-PL could not ameliorate the anorexia of CAC mice. Therefore, EPA-PL prevents cachectic weight loss in CAC mice, most likely by preservation of adipose tissue through inhibiting lipolysis.

Mechanisms of EPA-PL regulating lipolysis are multifactorial. As aforementioned, increased lipolysis of adipose tissue in CAC is related to lipolytic factors from the malignant tumor or host tissue. ZAG, a potent lipid mobilizing factor, is overexpressed by several types of malignant tumor. A number of studies have shown that treatment with purified ZAG can stimulate glycerol release in adipoctyes and causes body weight loss in obese and normal mice [16]. Our present data showed that the mRNA expression of ZAG in WAT of CAC mice

was up-regulated dramatically in the WAT of CAC mice but dietary EPA-PL decreased its mRNA level significantly. This result is in consistent with the previous study, which have also demonstrated that EPA may preserve adipose tissue in cachectic mice by down-regulation of ZAG expression [23]. In addition, It has been also suggested that TG lipases such as ATGL and HSL play an essential role in the pathogenesis of CAC [35]. In the process of lipolysis, the breakdown of TG which stored in WAT is mediated by ATGL and HSL. ATGL can convert TG into diacylglycerol and it is then hydrolyzed by HSL. Das *et al* [36] indicate that ATGL-deficient and HSL-deficient mice with tumor preserve adipose tissue as compared to normal cachectic mice and ATGL activity is increased significantly in the WAT of cancer cachectic patients. Our findings demonstrated that oral treatment of EPA-PL could markedly suppress the increased expression of ATGL and HSL in CAC mice. These results suggest that the anti-cachectic effects of EPA-PL in CAC mice are associated with regulation of lipolysis.

Some trials also demonstrate that the main cause of cancer cachexia is an inflammatory process [37]. Overexpression of pro-inflammatory cytokines such as TNF-α and IL-6 has been well established to play a crucial role in strong stimulation of lipolysis in CAC [5]. In this study we found that serum levels of TNF-α and IL-6 increased dramatically in CAC mice but decreased markedly after oral administration of EPA-PL. Reduction of pro-inflammatory cytokines secretion by EPA-PL might be attributed to prominent anti-inflammatory properties of EPA [38]. To confirm the antilipolytic effects of EPA-PL and further elucidate the possible mechanisms by which EPA-PL inhibits pro-inflammatory cytokines-induced lipolysis, we also employed TNF-α to stimulate the lipolysis of 3T3-L1 mature adipocytes. In the present

study, we did not observe antilipolytic effects of EPA-PL on basal lipolysis in 3T3-L1 adipocytes. However, EPA-PL could prevent the TNF-α-stimulated lipolysis after treatment of 48 h. In addition, our data also showed that an anti-diabetic drug rosiglitazone (an agonist of PPAR-γ), which has been suggested to be able to inhibit lipolysis in adipocytes [8], attenuated both basal and TNF-α-stimulated lipolysis significantly. These findings may prove that antilipolytic effects of EPA-PL is related to its anti-inflammatory properties. ERK 1/2 activation has been involved in the regulation of TNF-α-stimulated lipolysis in adipocytes. Previous studies have demonstrated that ERK 1/2 activation is important for promoting TNF-α-stimulated lipolysis by decreasing perilipin expression [8]. Some studies also reveal that activation of ERK 1/2 can mediate phosphorylation of PPAR-γ and reduce its transcriptional activity [39]. Our present data showed that antilipolytic effects of EPA-PL boosted notably in the presence of PD 98059 (an inhibitor of ERK 1/2). Moreover, a recent study also suggests that EPA can prevent TNF-α-induced ERK 1/2 phosphorylation in preadipocytes and adipocytes [30]. These findings indicate that the inhibitory effects of EPA-PL on TNF-α-induced ERK 1/2 activation may account for its antilipolytic action in adipocytes. In addition, a wealth of studies have suggested that AMPK also play a pivotal role in lipolysis [9]. As far as we know, most of studies report that activation AMPK can inhibit lipolysis [40,41]. However, others have manifested that AMPK phosphorylates and activates ATGL, then increases lipolysis [42]. Thus, the effects of AMPK activation on lipolysis are controversial. This controversial results might be explained by time dependence [43]. Our present data showed that AICAR-induced AMPK activation could suppress the basal and TNF-α-stimulated

lipolysis in 3T3-L1 adipocytes, which support the former suggestion. Moreover, the antilipolytic action of EPA-PL on TNF-α-stimulated lipolysis was blocked by compound C (an inhibitor of AMPK), suggesting that the antilipolytic action of EPA-PL in adipocytes is also regulated by the activation of AMPK. On the other hand, it has been observed that activation of PI3K/Akt pathways is also important for mediating lipolysis in adipocytes [44]. PI3K is a major player of insulin action, and its activation increases dephosphorylation of HSL and then inhibition of lipolysis [10]. Our present data showed that the presence of PI3K inhibitor LY294002 abrogated the antilipolytic action of EPA-PL on TNF-α-stimulated lipolysis in adipocytes. It indicates that the antilipolytic effects of EPA-PL could be mediated via activation of PI3K/Akt pathways.

In addition to increased lipolysis, lipid over-utilization is also considered as being responsible for the pathogenesis of cachexia. And it has been observed that prior to skeletal muscle atrophy, a phenotypic switched from WAT to BAT (which is also called WAT browning) occurs and increases energy expenditure in several CAC mice models [9,45]. Hence, inhibition of WAT browning might preserve WAT mass and rescue the cachexia. As we know, PGC-1α, a key regulator in energy metabolism, is expressed at low levels in WAT but is abundant in metabolically active tissues such as BAT [13]. It has been reported that the mRNA level of PGC-1α is overexpressed in the WAT of CAC mice [14], suggesting the development of WAT browning in CAC mice. UCP2, a mitochondrial anion carrier proteins, also involves in regulation of lipid utilization [46]. Moreover, a study also demonstrates that treatment with ZAG in mice leads to an up-regulation of UCP2 mRNA [47]. Our present

findings showed that the mRNA levels of PGC-1α and UCP2 in WAT were up-regulated significantly in CAC mice resulting in the enhancement of the mitochondrial activities converting WAT into BAT and then increasing lipid utilization. Dietary EPA-PL could reverse these increases, suggesting ameliorating effects of EPA-PL in CAC mice through suppressing the lipid over-utilization.

As has been mentioned above, excessive loss of adipose mass is also attributable to a decrease in lipid deposition. Adipogenesis which involves preadipocyte differentiation and adipocyte maturation in adipose tissue is also impeded in the process of CAC. The observation manifests that the mRNA expression of several key adipogenic transcription factors such as C/EBP α, C/EBP β, PPAR γ and SREBP-1c are suppressed in the WAT of CAC mice [14]. Several studies have demonstrated the effects of EPA on adipogenesis. However, the effects described for EPA on adipogenesis are controversial, showing promotion [48] and suppression of adipogenesis [49,50] in adipocytes. In the present study we did not observe any significant effects of EPA-PL on 3T3-L1 preadipocytes differentiation after incubated for 48 h. Our data also found that oral administration of EPA-PL did not affect the mRNA expression of these key adipogenic transcription factors in WAT of CAC mice except for C/EBP α. Furthermore, it is also observed that LPL and glucose GLUT4 play a part in the anabolic process of adipogenesis [20,21]. Some evidences show that the reduction of LPL and GLUT4 mRNA levels are involved in cachexia [14,35] . Moreover, LPL is regulated by C/EBP α and PPAR γ in fatty acid metabolism [51]. Our present results demonstrated that the genes of LPL and GLUT4 were dramatically inhibited in the WAT of CAC mice. But treatment of

EPA-PL could increase the mRNA levels of these genes. All these data suggest that the ability of EPA-PL to preserve adipose mass in CAC mice could also contribute to recovering the function of adipogenesis.

5 Conclusion

In summary, our findings in this study provide evidences that dietary EPA-PL ameliorates CAC mainly via inhibiting lipolysis. The antilipolytic effects of EPA-PL *in vivo* and *in vitro* is due to its anti-inflammatory properties, inhibition the expression of lipid mobilizing factor and key rate limiting lipases, inactivation of ERK 1/2 as well as activation of AMPK and PI3K. Oral administration of EPA-PL also prevents the white adipose tissue browning in CAC mice, thus decreases lipid over-utilization. In addition, our present study also observes that the anti-cachectic effects of EPA-PL are at least partly responsible for recovering the function of adipogenesis in CAC mice. Although further investigations are warranted to confirm the structure-activity relationship of phospholipids type or the variety of PUFAs, these encouraging findings may provide the basis for marine phospholipids supplementation in cancer-associated cachexia therapy.

Acknowledgments

This work was supported by the grants form National Natural Science Foundation of China (NSFC)-Shandong Joint Fund for Marine Science Research Centers (U1406402), NSFC (31371757, 31201329), the Program for New Century Excellent Talents in University (NCET-13-0534) and the Towa Foundation for Food Science & Research. The author Lei Du

also thanks China Scholarship Council (No. 201206330082) for supporting his study in Hokkaido University.

References

1 J. M. Argilés, R. Moore-Carrasco, G. Fuster, S. Busquets and F. J. López-Soriano, *Int. J. Biochem. Cell Biol.*, 2003, **35**, 405-409.

2 M. Rydén, T. Agustsson, J. Laurencikiene, T. Britton, E. Sjölin, B. Isaksson, J. Permert and P. Arner, *Cancer*, 2008, **113**, 1695-704.

3 M. Rydén and P. Arner, *Clin. Nutr.*, 2007, **26**, 1-6.

4 R. Zimmermann, J. G. Strauss, G. Haemmerle, G. Schoiswohl, R. Birner-Gruenberger, M. Riederer, A. Lass, G. Neuberger, F. Eisenhaber, A. Hermetter and R. Zechner, *Science*, 2004, **306**, 1383-1386.

5 M. J. Tisdale, *Physiol. Rev.*, 2009, **89**, 381-410.

6 M. Rydén, E. Arvidsson, L. Blomqvist, L. Perbeck, A. Dicker and P. Arner, *Biochem. Biophys. Res. Commun.*, 2004, **318**, 168-175.

7 H. H. Zhang, M. Halbleib, F. Ahmad, V. C. Manganiello and A. S. Greenberg, *Diabetes*, 2002, **51**, 2929-2935.

8 S. C. Souza, H. J. Palmer, Y. H. Kang, M. T. Yamamoto, K. V Muliro, K. E. Paulson and A. S. Greenberg, *J. Cell. Biochem.*, 2003, **89**, 1077-1086.

9 M. Daval, *J. Biol. Chem.*, 2005, **280**, 25250-25257.

10 M. Ridderstråle, *Curr. Drug Targets. Immune. Endocr. Metabol. Disord.*, 2005, **5**, 79-92.

11 M. Petruzzelli, M. Schweiger, R. Schreiber, R. Campos-Olivas, M. Tsoli, J. Allen, M. Swarbrick, S. Rose-John, M. Rincon, G. Robertson, R. Zechner and E. F. Wagner, *Cell Metab.*, 2014, **20**, 433-447.

12 S. Kir, J. P. White, S. Kleiner, L. Kazak, P. Cohen, V. E. Baracos and B. M. Spiegelman, *Nature*, 2014, **513**, 100-104.

13 H. Liang and W. F. Ward, *Adv. Physiol. Educ.*, 2006, **30**, 145-151.

14 C. Bing, S. Russell, E. Becket, M. Pope, M. J. Tisdale, P. Trayhurn and J. R. Jenkins, *Br. J. Cancer*, 2006, **95**, 1028-1037.

15 D. Ricquier and F. Bouillaud, *Biochem. J.*, 2000, **345 Pt 2**, 161-179.

16 C. Bing and P. Trayhurn, *Proc. Nutr. Soc.*, 2009, **68**, 385-392.

17 T. H. Chung, M. Y. P Kuo, J. K. Chen and D. M. Huang, *Int. J. Cancer*, 2011, **129**, 2274-2283.

18 E. D. Rosen, *Prostaglandins, Leukot. Essent. Fat. Acids*, 2005, **73**, 31-34.

19 J. D. Horton, *Biochem Soc Trans.*, 2002, **30**, 1091-1095.

20 J. R. Mead, S. A. Irvine and D. P. Ramji, *J. Mol. Med. (Berl).*, 2002, **80**, 753-769.

21 M. E. Fernyhough, E. Okine, G. Hausman, J. L. Vierck and M. V. Dodson, *Domest. Anim. Endocrinol.*, 2007, **33**, 367-378.

22 M. J. Tisdale and S. A. Beck, *Biochem. Pharmacol.*, 1991, **41**, 103-107.

23 S. T. Russell and M. J. Tisdale, *Prostaglandins. Leukot. Essent. Fatty Acids*, 2005, **72**, 409-414.

24 A. Giacosa and M. Rondanelli, *Genes Nutr.*, 2008, **3**, 25-28.

25 T. T. Brown, D. L. Zelnik and A. S. Dobs, *Int. J. Gastrointest. Cancer*, 2003, **34**, 143-150.

26 J. Folch, M. Lees and G.H. Sloane Stanley, *J. Biol. Chem.*, 1957, **226**, 497-509.

27 Z. Hossain, H. Kurihara, M. Hosokawa and K. Takahashi, *Mol. Cell. Biochem.*, 2006, **285**, 155-163.

28 A.F. Prevot and F.X. Mordred, *Rev. Fr. Corps Gras.*, 1976, **23**, 409-423.

29 E. G. Hong, H. J. Ko, Y. R. Cho, H. J. Kim, Z. Ma, T. Y. Yu, R. H. Friedline, E. Kurt-Jones, R. Finberg, M. A. Fischer, E. L. Granger, C. C. Norbury, S. D. Hauschka, W. M. Philbrick, C. G. Lee, J. A. Elias and J. K. Kim, *Diabetes*, 2009, **58**, 2525-2535.

30 S. Lorente-Cebrián, M. Bustos, A. Marti, M. Fernández-Galilea, J. A. Martinez and M. J. Moreno-Aliaga, *J. Nutr. Biochem.*, 2012, **23**, 218-227.

31 L. A. Taylor, L. Pletschen, J. Arends, C. Unger and U. Massing, *Support. Care Cancer*, 2010, **18**, 159-170.

32 F. S. H. Lu, N. S. Nielsen, M. Timm-Heinrich and C. Jacobsen, *Lipids*, 2011, **46**, 3-23.

33 B. Goustard-Langelier, P. Guesnet, G. Durand, J. M. Antoine and J. M. Alessandri, *Lipids*, 1999, **34**, 5-16.

34 V. Wijendran, M. C. Huang, G. Y. Diau, G. Boehm, P. W. Nathanielsz and J. T. Brenna, *Pediatr. Res.*, 2002, **51**, 265-272.

35 S. K. Das and G. Hoefler, *Trends Mol. Med.*, 2013, **19**, 292-301.

36 S. K. Das, S. Eder, S. Schauer, C. Diwoky, H. Temmel, B. Guertl, G. Gorkiewicz, K. P. Tamilarasan, P. Kumari, M. Trauner, R. Zimmermann, P. Vesely, G. Haemmerle, R. Zechner and G. Hoefler, *Science (80-.).*, 2011, **333**, 233-238.

37 M. J. Tisdale, *J. Cell. Biochem.*, 2004, **93**, 871-877.

38 P. Pérez-Matute, N. Pérez-Echarri, J. A. Martínez, A. Marti and M. J. Moreno-Aliaga, *Br. J. Nutr.*, 2007, **97**, 389-398.

39 E. Hu, J. B. Kim, P. Sarraf and B. M. Spiegelman, *Science*, 1996, **274**, 2100-2103.

576 40 N. M. Anthony, M. P. Gaidhu and R. B. Ceddia, *Obesity (Silver Spring).*, 2009, **17**, 1312-1317.

578 41 Y. Dagon, Y. Avraham and E. M. Berry, *Biochem. Biophys. Res. Commun.*, 2006, **340**, 43-47.

580 42 M. Ahmadian, M. J. Abbott, T. Tang, C. S. S. Hudak, Y. Kim, M. Bruss, M. K. Hellerstein, H. Y. Lee, V. T. Samuel, G. I. Shulman, Y. Wang, R. E. Duncan, C. Kang and H. S. Sul, *Cell Metab.*, 2011, **13**, 739-748.

583 43 W. Yin, J. Mu and M. J. Birnbaum, *J. Biol. Chem.*, 2003, **278**, 43074-43080.

584 44 M. Fernandez-Galilea, P. Perez-Matute, P. L. Prieto-Hontoria, J. a. Martinez and M. J. Moreno-Aliaga, *J. Lipid Res.*, 2012, **53**, 2296-2306.

586 45 D. Holmes, *Nat. Rev. Endocrinol.*, 2014, **10**, 578.

587 46 O. Boss, T. Hagen and B. B. Lowell, *Diabetes*, 2000, **49**, 143-156.

588 47 C. Bing, S. T. Russell, E. E. Beckett, P. Collins, S. Taylor, R. Barraclough, M. J. Tisdale and G. Williams, *Br. J. Cancer*, 2002, **86**, 612-618.

590 48 G. Murali, C. V Desouza, M. E. Clevenger, R. Ramalingam and V. Saraswathi, *Prostaglandins Leukot. Essent. Fat. Acids*, 2014, **90**, 13-21.

592 49 M. S. Lee, I. S. Kwun and Y. Kim, *Genes Nutr.*, 2008, **2**, 327-330.

50 L. Madsen, R. K. Petersen and K. Kristiansen, *Biochim. Biophys. Acta*, 2005, **1740**, 266-286.

51 M. J. Yim, M. Hosokawa, Y. Mizushina, H. Yoshida, Y. Saito and K. Miyashita, *J. Agric. Food Chem.*, 2011, **59**, 1646-1652.

Figure captions and Table

Fig. 1 Effects of EPA-PL on mRNA expression of lipolysis genes in the WAT of CAC mice. The mRNA expressions of ZAG, ATGL and HSL in the WAT of mice received oral treatments with normal saline or EPA-PL (100 mg/kg/day) for totally 14 consecutive days were measured by real-time PCR. Data normalization was accomplished using the endogenous reference β-actin. Values are expressed as mean ± SEM (n = 8), $^{\#}P < 0.05$, $^{\#\#}P < 0.01$ versus normal control mice, $^{*}P < 0.05$, $^{**}P < 0.01$ versus model control mice.

Fig. 2 Effects of EPA-PL on mRNA expression of lipid utilization genes in the WAT of CAC mice. The mRNA levels of PGC-1α and UCP 2 in the WAT of mice received oral administration of normal saline or EPA-PL (100 mg/kg/day) for 14 consecutive days were measured by real-time PCR. Data normalization was accomplished using the endogenous reference β-actin. Values are expressed as mean ± SEM (n = 8), $^{\#}P < 0.05$, $^{\#\#}P < 0.01$ versus normal control mice, $^{*}P < 0.05$, $^{**}P < 0.01$ versus model control mice.

Fig. 3 Effects of EPA-PL on mRNA expression of adipogenic genes in the WAT of CAC mice. The mRNA expressions of adipogenic factors involved in preadipocyte differentiation and adipocyte maturation in the WAT of mice received oral administration of normal saline or EPA-PL (100 mg/kg/day) for 14 consecutive days were measured by real time PCR. Data normalization was accomplished using the endogenous reference β-actin. Values are expressed as mean ± SEM (n = 8), $^{\#}P < 0.05$, $^{\#\#}P < 0.01$ versus normal control mice, $^{*}P < 0.05$, $^{**}P < 0.01$ versus model control mice.

Fig. 4 EPA-PL inhibits TNF-α-stimulated lipolysis in 3T3-L1 adipocytes. (A) Effects of EPA-PL on proliferation of 3T3-L1 adipocytes. 3T3-L1 adipocytes were treated with various

concentrations of EPA-PL for 48 h. Control cells were treated with the same amount of ethanol (EtOH). Values are expressed as mean ± SEM of three independent experiments. (B) Effects of EPA-PL on TNF-α-stimulated lipolysis was assessed by Oil Red O staining. After differentiation for 8 days, 3T3-L1 mature adipocytes were treated with 10 ng/mL TNF-α in the presence or absence of 200 μM EPA-PL for 48 h. The lipid accumulation in lipid droplets was examined by Oil Red O staining.

Fig. 5 Effects of EPA-PL (200 and 400 μM) and rosiglitazone (10, 25 and 50 μM) on basal (A) and TNF-α-stimulated lipolysis (B) in 3T3-L1 adipocytes for 48 h. Lipolysis was evaluated by measuring the amount of glycerol released into media. The cells were rinsed with ice-cold PBS, harvested and lysed by lysis buffer. Protein concentrations in the lysates were used to normalize the lipolysis signals. Values are expressed as mean ± SEM (n = 6), $^{\#}P < 0.05$, $^{\#\#}P < 0.01$ versus control cells; $^{*}P < 0.05$, $^{**}P < 0.01$ versus TNF-α-treated cells; $^{a}P < 0.05$ versus TNF-α in combination with EPA-PL (400 μM).

Fig. 6 Effects of EPA-PL (200 μM) on basal (A) and TNF-α-stimulated lipolysis (B) in 3T3-L1 adipocytes alone or in the presence of AMPK activator AICAR (1 mM), AMPK inhibitor compound C (20 μM), PI3K inhibitor LY 294002 (50 μM) and ERK 1/2 inhibitor PD 98059 (50 μM) for 48 h. Lipolysis was evaluated by measuring the amount of glycerol released into media. The cells were rinsed with ice-cold PBS, harvested and lysed by lysis buffer. Protein concentrations in the lysates were used to normalize the lipolysis signals. Values are expressed as mean ± SEM (n = 6), $^{\#}P < 0.05$, $^{\#\#}P < 0.01$ versus control cells; $^{*}P < 0.05$, $^{**}P < 0.01$ versus TNF-α-treated cells; $^{a}P < 0.05$ versus TNF-α in combination with EPA-PL.

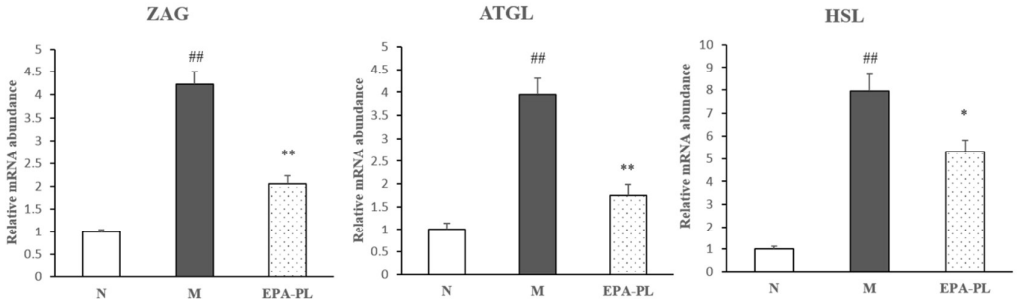

Fig. 1 Effects of EPA-PL on mRNA expression of lipolysis genes in the WAT of CAC mice.

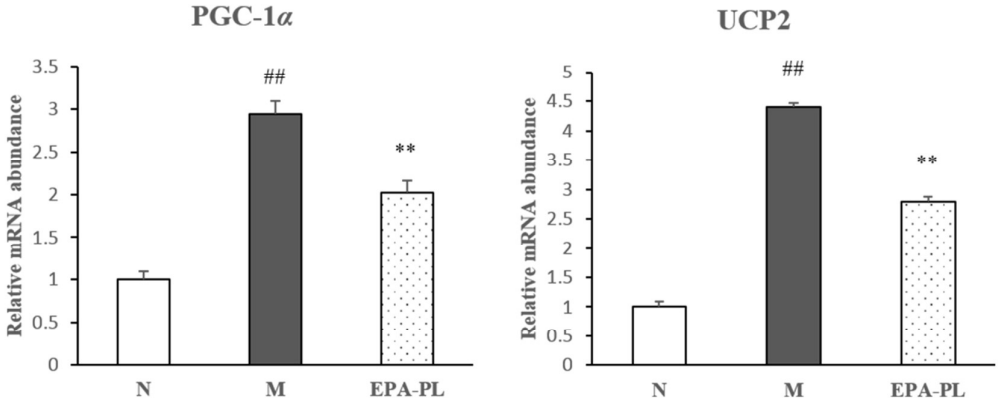

Fig. 2 Effects of EPA-PL on mRNA expression of lipid utilization genes in the WAT of CAC mice.

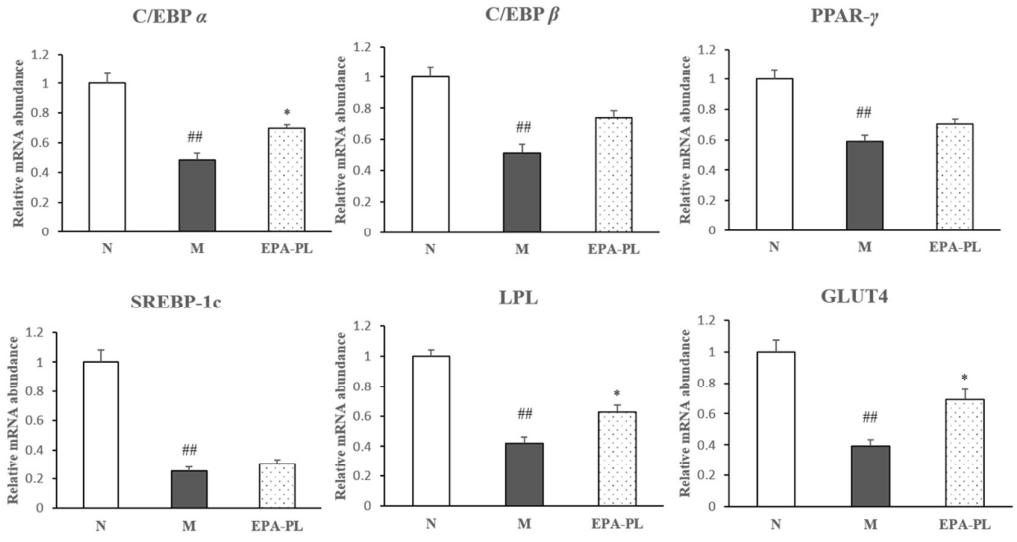

Fig. 3 Effects of EPA-PL on mRNA expression of adipogenic genes in the WAT of CAC mice.

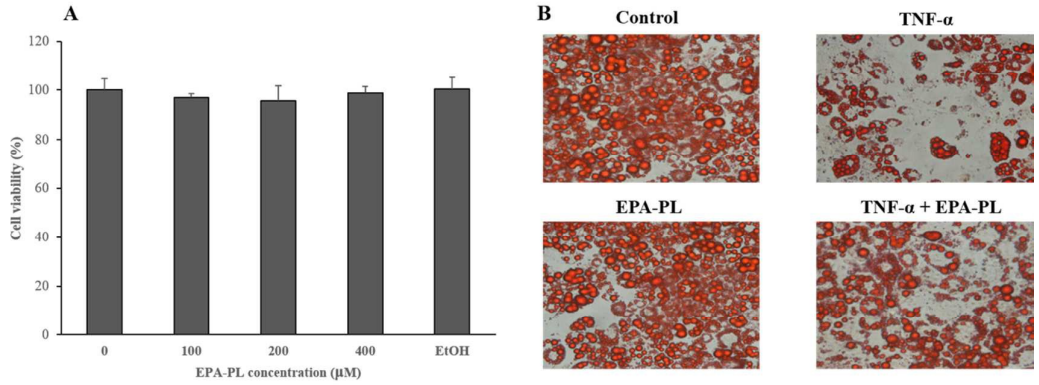

Fig. 4 EPA-PL inhibits TNF-α-stimulated lipolysis in 3T3-L1 adipocytes. (A) Effects of EPA-PL on proliferation of 3T3-L1 adipocytes. (B) Effects of EPA-PL on TNF-α-stimulated lipolysis was assessed by Oil Red O staining.

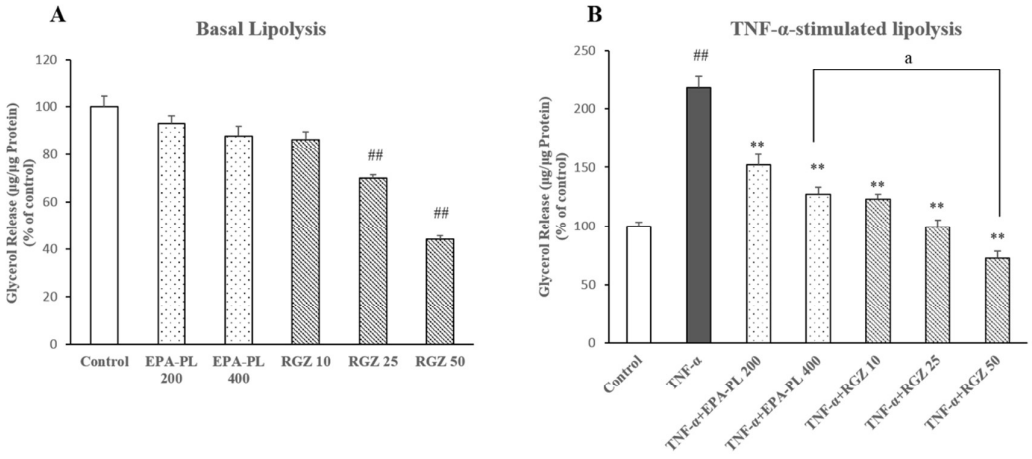

Fig. 5 Effects of EPA-PL (200 and 400 μM) and rosiglitazone (10, 25 and 50 μM) on basal (A) and TNF-α-stimulated lipolysis (B) in 3T3-L1 adipocytes for 48 h.

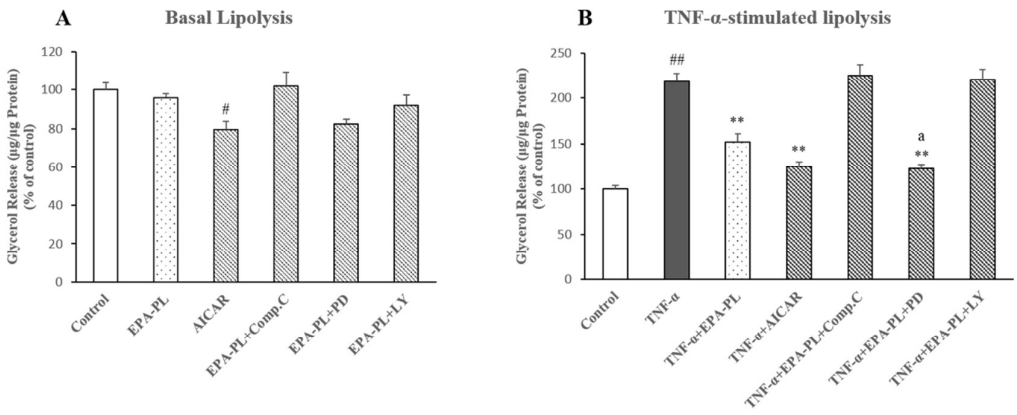

Fig. 6 Effects of EPA-PL (200 μM) on basal (A) and TNF-α-stimulated lipolysis (B) in 3T3-L1 adipocytes alone or in the presence of AMPK activator AICAR (1 mM), AMPK inhibitor compound C (20 μM), PI3K inhibitor LY 294002 (50 μM) and ERK 1/2 inhibitor PD 98059 (50 μM) for 48 h.

Table 1 Sequences of the primers used in the study

Gene name	Accession No.	Forward primer	Reverse primer
ZAG	NM_013478	GCCTGTCCTGCTGTCCCT	CTCCCAGTCCTCCATTCCT
ATGL	AY894805	ACTGAACCAACCCAACCCT	GCAGCCACTCCAACAAGC
HSL	U08188.1	GAGAACCGCTAAGCATCCC	GCCAACCAAGTATTCAAACCTA
C/EBP α	NM_007678	GGACACGGGGACCATTAG	CTGGGAGGCAGACGAAAA
C/EBP β	NM_009883	GCTGACGGCGGAGAACGA	CATCAAGTCCCGAAACCC
PPAR γ	AY243585	GTGATGGAAGACCACTCGC	CCCACAGACTCGGCACTC
SREBP-1c	NM_011480	AAACTGCCCATCCACCGAC	GCCTCCTCCACTGCCACA
PGC-1α	NM_008904	AGGTCCCCAGGCAGTAGAT	GAGCAGCGAAAGCGTCAC
UCP2	U69135.1	CTGGTGGTGGTCGGAGAT	GCAGAAGTGAAGTGGCAAGG
GLUT4	AB008453	ACTAAGAGCACCGAGACCAA	CTGCCCGAAAGAGTCTAAAG
LPL	NM_008509	GAGTTTGACCGCCTTCCG	TCCCGTTACCGTCCATCC
β-actin	NM_007393	CAGGCATTGCTGACAGGATG	TGCTGATCCACATCTGCTGG

Table 2 Fatty acid composition of EPA-PL extracted from starfish

Fatty acid composition (%)	EPA-PL
C14:0	0.71 ± 0.01
C16:0	3.40 ± 0.23
C16:1	3.19 ± 0.18
C18:0	8.52 ± 0.32
C18:1	6.51 ± 0.31
C20:1	5.57 ± 0.15
C20:2	0.51 ± 0.33
C20:3	0.09 ± 0.06
C20:4 n-6 (AA)	8.85 ± 0.07
C20:5 n-3 (EPA)	42.0 ± 0.83
C22:6 n-3 (DHA)	6.84 ± 0.41
Others	13.8
∑SFA	12.6
∑MUFA	15.2
∑PUFA	58.2
∑n-3 PUFA	48.8

Table 3 Effects of EPA-PL on physiological, serum parameters and serum cytokines in mice

Physiological parameters	**Normal**	**Model**	**EPA-PL**
Average food intake (g/day)	4.08 ± 0.38	2.32 ± 0.41[b]	2.31 ± 0.48
Carcass weight (g)	27.3 ± 0.87	21.2 ± 1.16[b]	24.6 ± 1.03[d]
WAT mass (g)	0.99 ± 0.07	0.44 ± 0.03[b]	0.62 ± 0.03[d]
Serum parameters	**Normal**	**Model**	**EPA-PL**
NEFA (mmol/L)	1.05 ± 0.06	1.94 ± 0.11[b]	1.29 ± 0.06[d]
Serum cytokines	**Normal**	**Model**	**EPA-PL**
TNF-α (pg/mL)	9.34 ± 0.91	44.6 ± 2.06[b]	21.0 ± 2.25[d]
IL-6 (pg/mL)	10.6 ± 0.95	15.2 ± 1.04[b]	8.93 ± 1.07[d]

Each value represents a mean ± SEM (n = 8). [a]$P < 0.05$, [b]$P < 0.01$ versus normal control, [c]$P < 0.05$, [d]$P < 0.01$ versus model control.

Graphical abstract

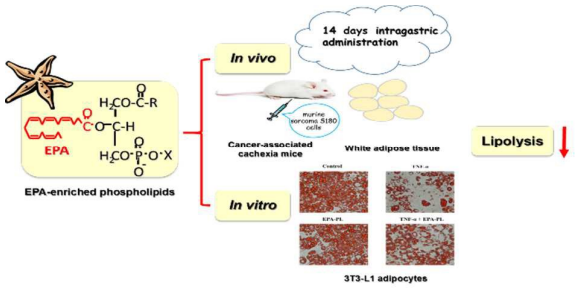

EPA-PL rescues the cancer-associated cachexia via inhibiting lipolysis